# Topologically structured sensors with high linearity and decoupling dual-sensing signals

Huanyu Liu[a], Chengkai Luo[a], Yunhui Wu[a]*, Xinxing Zhang[b]

a. School of Mechanical Engineering & College of Materials Science and Engineering, Dongguan University of Technology, Dongguan 523808, P. R. China

b. State Key Laboratory of Polymer Materials Engineering Polymer Research Institute of Sichuan University, Chengdu 610065, P. R. China

**Corresponding authors:**

Yunhui Wu: ***wuyh@dgut.edu.cn***

**Table S1.** Comparison of the sensing properties with other state-of-the-art multifunctional wearable sensors based on ILs.

| Material | Humidity Response /Sensitivity | Strain low limit /Response range | External stimulus detecting | Decoupled | References |
|---|---|---|---|---|---|
| TPU/ILs | NO | 10%/50% | Strain/temperature | YES | 1 |
| TPU/ILs parallel fiber | N0 | 0.1%/200 % | Strain/temperature | NO | 2 |
| PS-r-PnBMA/ ILs | NO | 10%/300 % | Strain/temperature | YES | 3 |
| Fabric/GO | YES/- | -/30% | Strain/temperature/ humidity | NO | 4 |
| PVA/CA/Ag | YES/- | 1%/200% | Strain/temperature/ humidity | NO | 5 |
| poly(lipoic acid | YES/0.89% | -/100% | Temperature/strain/ humidity | NO | 6 |
| TPU/ILs | YES/1.08% | - | Humidity/Press | YES | 7 |
| PILs | NO | -/300% | Strain/Temperature | NO | 8 |
| TPU/ILs/WP U | YES/12.4% | 0.1%/300 % | Strain/Temperature/ Humidity | YES | **This work** |

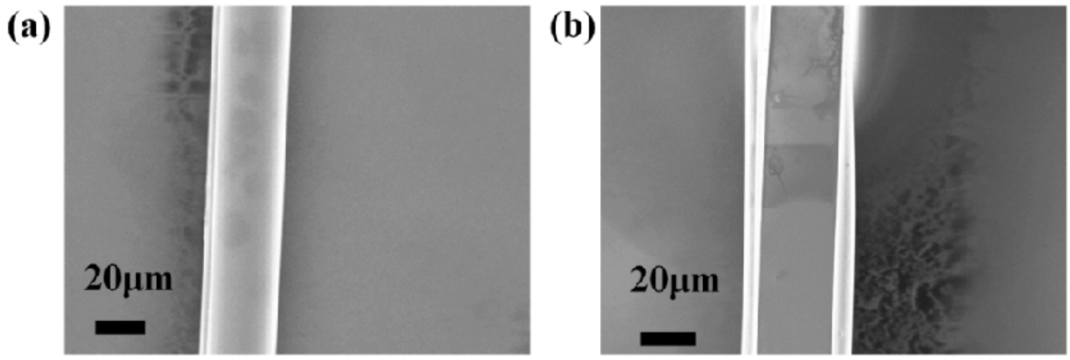


**Figure S1.** (a)  SEM image of PU, (b) SEM image of PU/ILs/WPU.

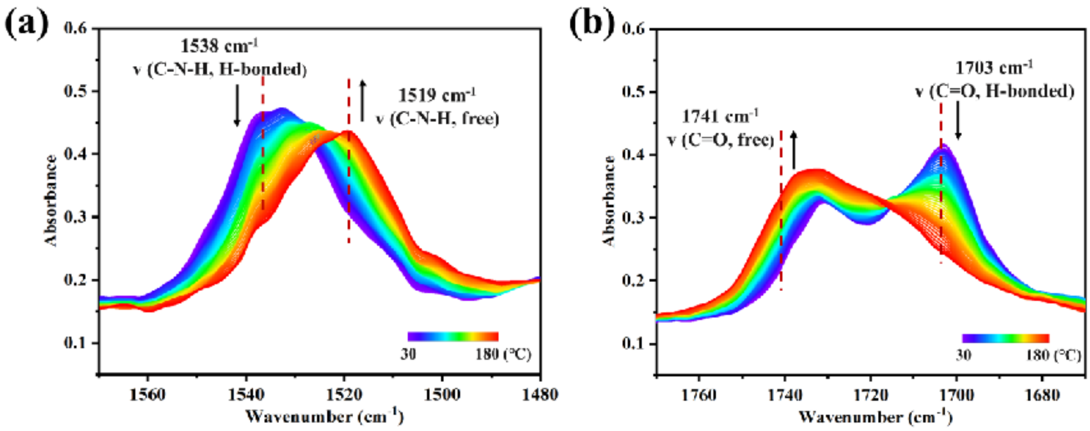


**Figure S2.** Temperature-dependent FTIR spectra of PU/ILs/WPU up heating from 30 to 180 °C, (a) 1480-1560 $cm^{-1}$, (b) 1680-1760 $cm^{-1}$.

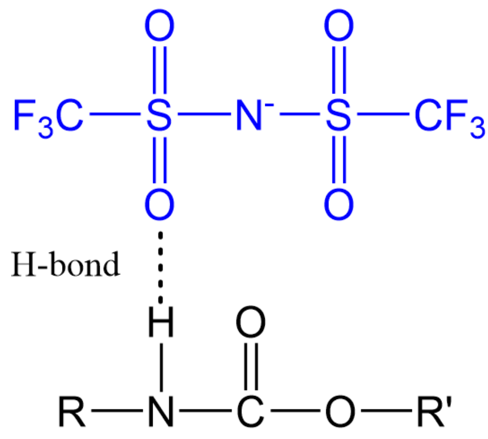


**Figure S3.** Schematic diagram of hydrogen bonding between PU and ILs.

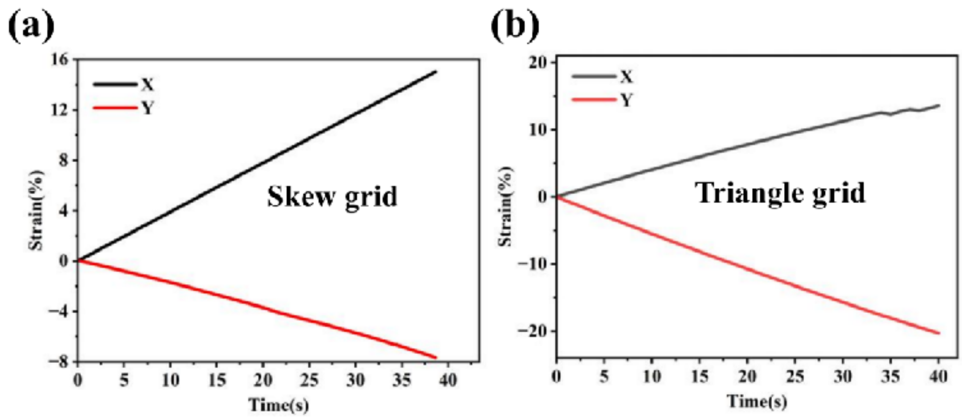


**Figure S4**. (a)The X-Y displacement variation of skew PU grid under stretching, (b)The X-Y displacement variation of triangle PU grid under stretching

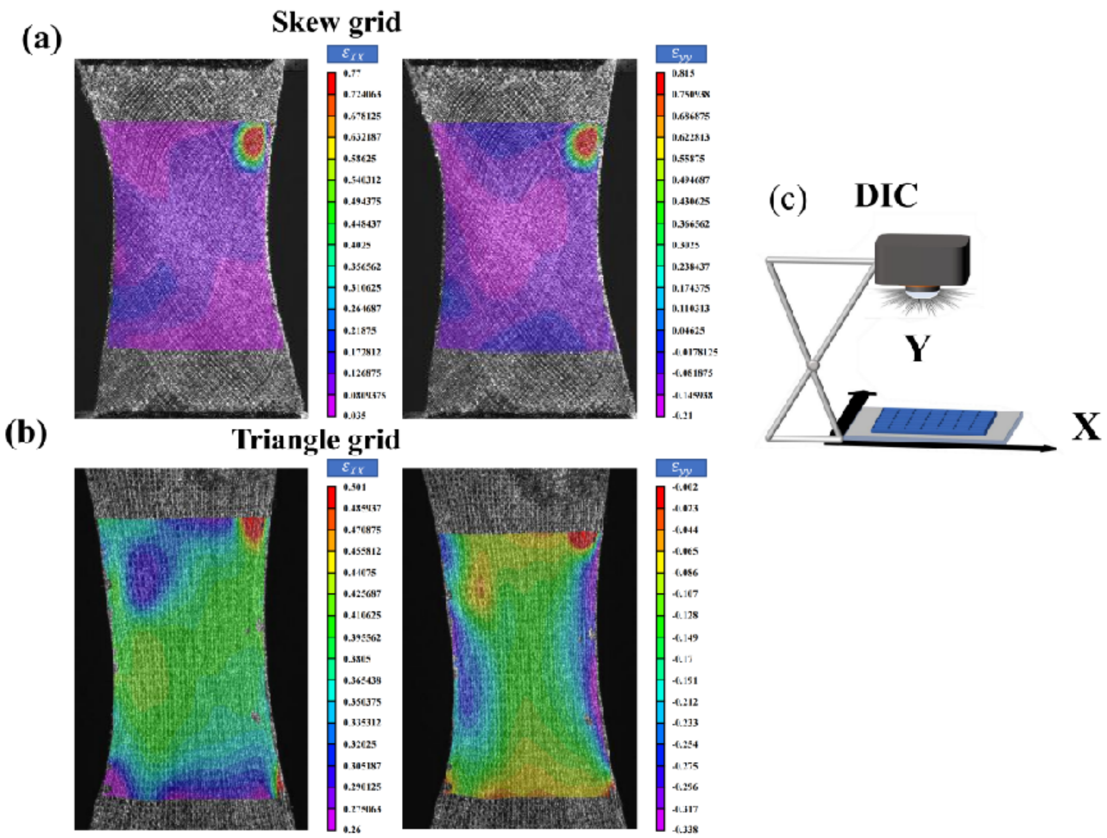


Figure S5. The DIC images of PU grid after stretching:(a)Skew grid,(b)triangle grid, (c) Schematic image of DIC

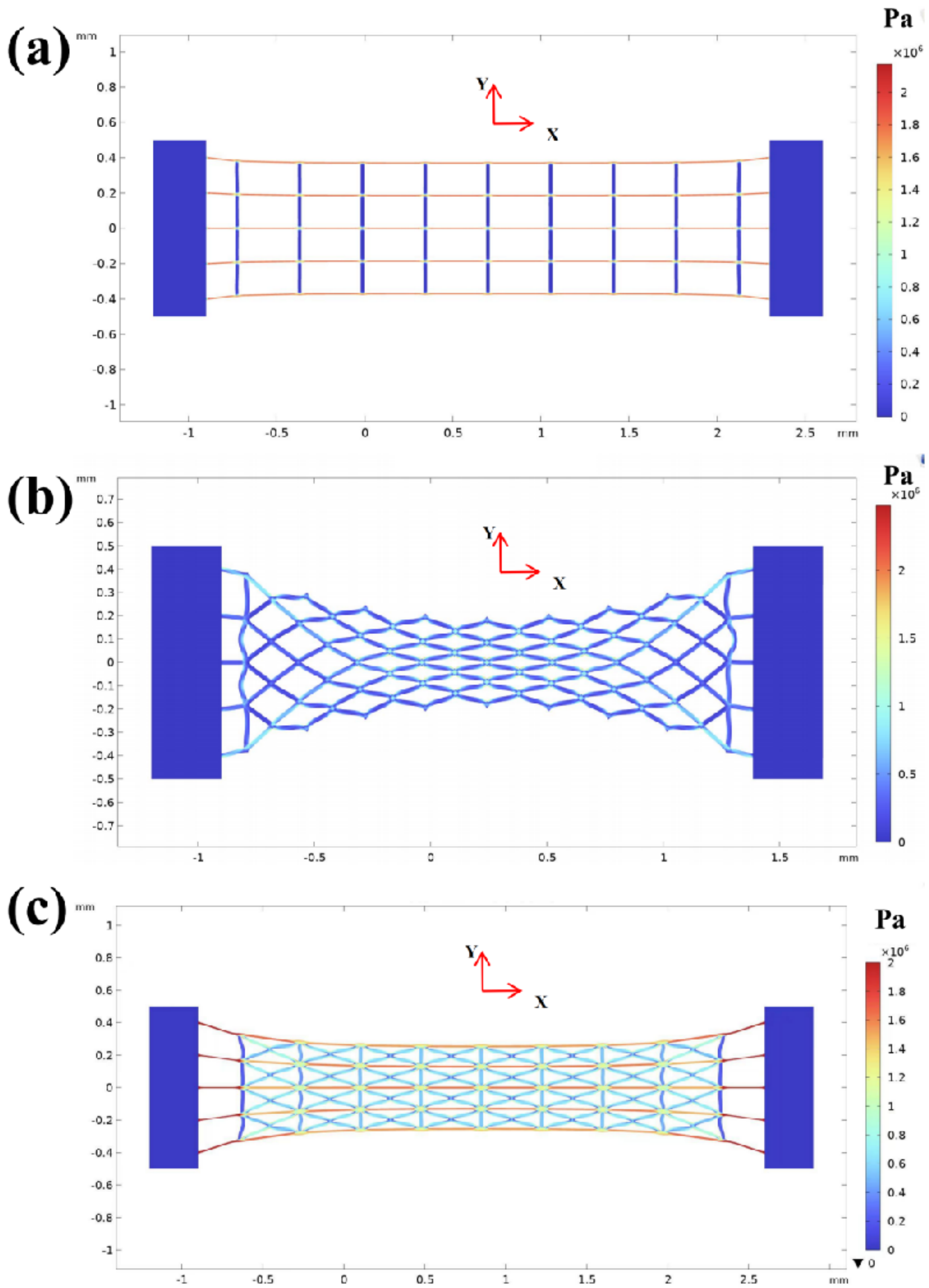


Figure S6. Stress-strain distribution simulation of stretched grid :(a) square grid at a scale factor of 3.5, (b) skew grid at a scale factor of 1.216, (c) triangle grid at a scale factor of 3.5.

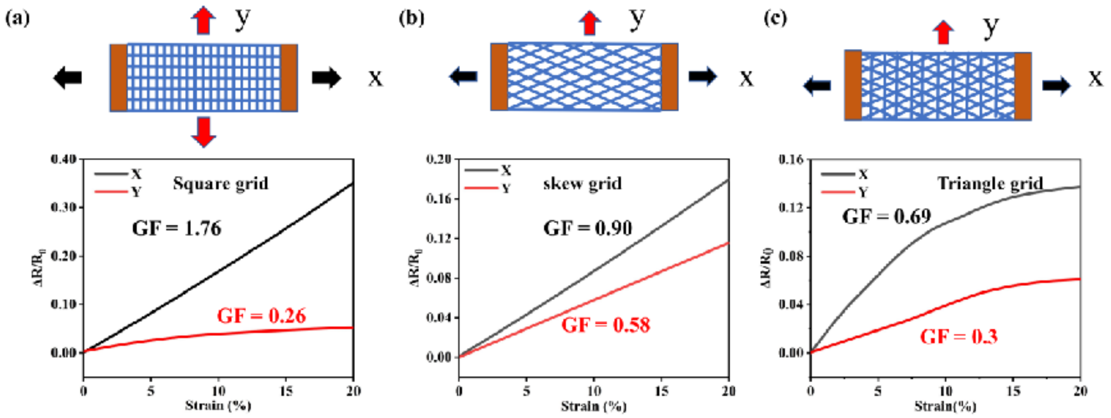


**Figure S7.** The $\Delta R/R_0$ of square grid，triangle grid, skew grid along x and y-axis stretching direction

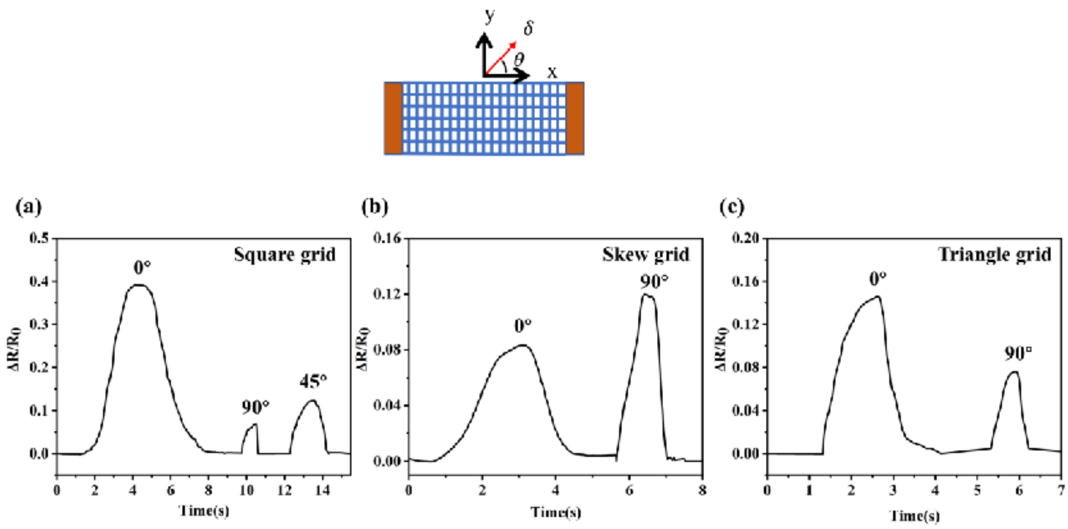


**Figure S8.** The resistance changes of grid sensors changing with the stretching angles (θ)

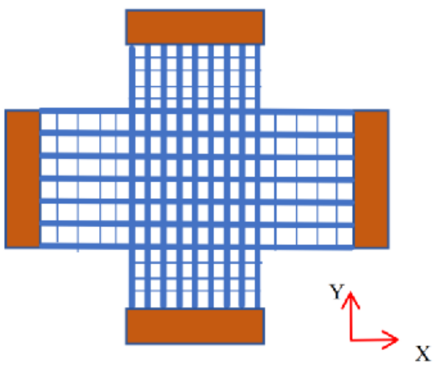

**Figure S9.** Schematic diagram of orthogonal stacking two grid strain sensors

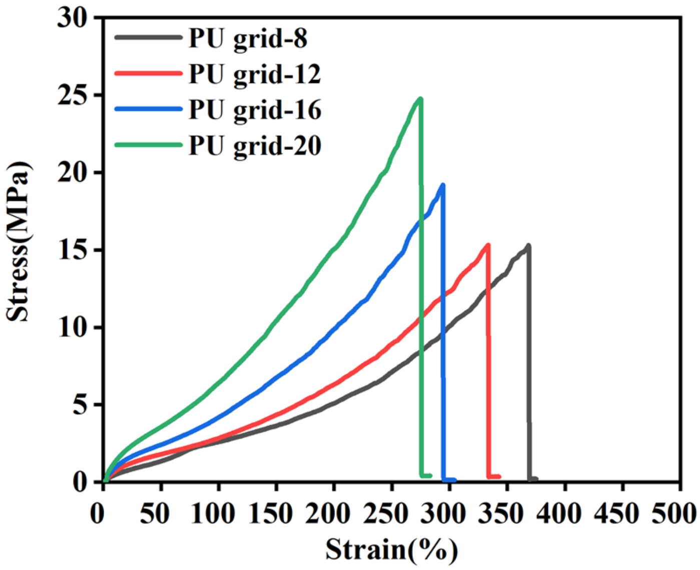


**Figure S10.** Stress-strain of PU grid with different layers.

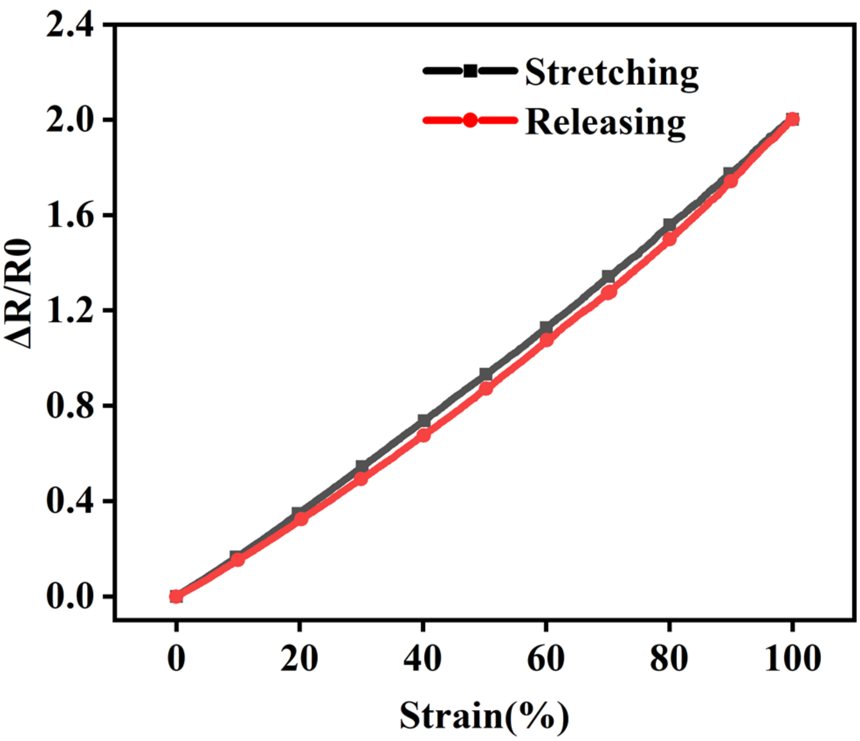

**Figure S11**. The resistance changes of square grid sensor during stretching-releasing

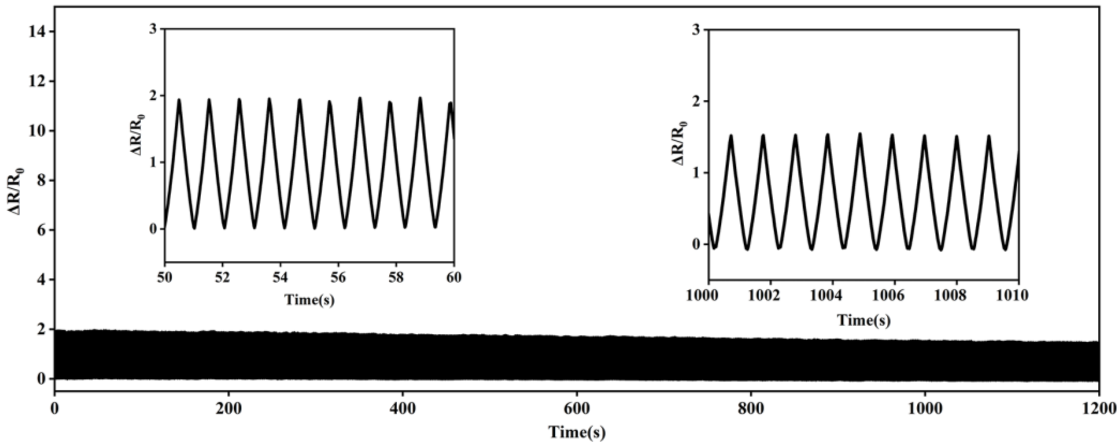


**Figure S12.** The resistance signals after 1200 stretching/releasing cycles.

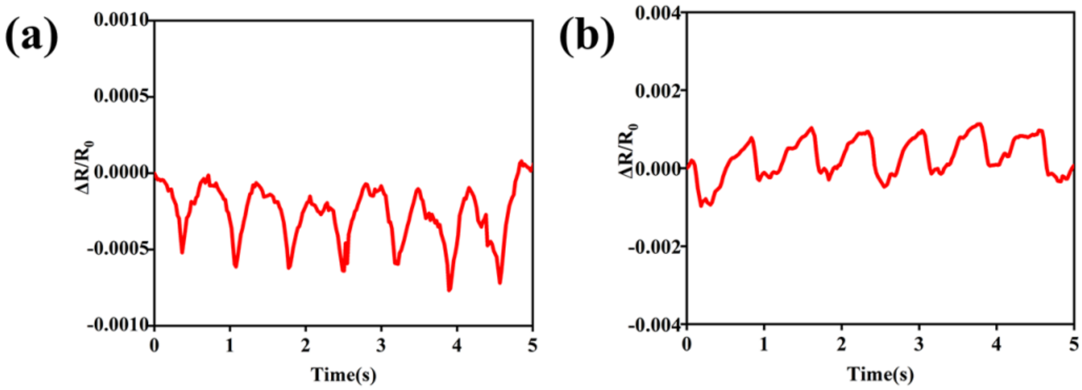


**Figure S13.** (a) Real-time monitoring of adult heart pulse, (b) Real-time monitoring of adult wrist pulse.

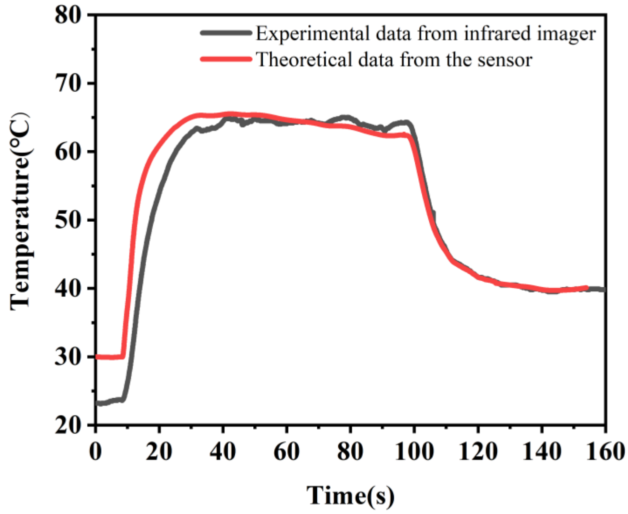


**Figure S14.** The comparison between experimental temperature and theoretical temperature from the resistance signal of senor.

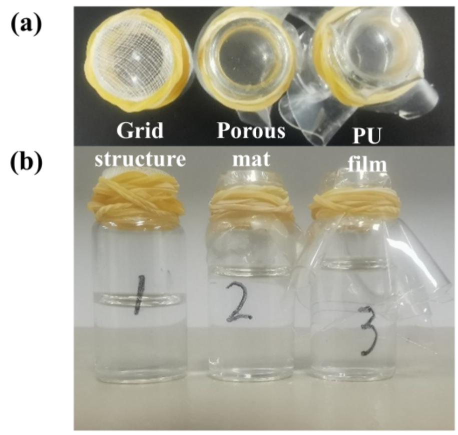


**Figure S15.** Permeability test picture: (a) Bottle caps of membrane, (b) The remaining water after stored in room temperature for 28 days.

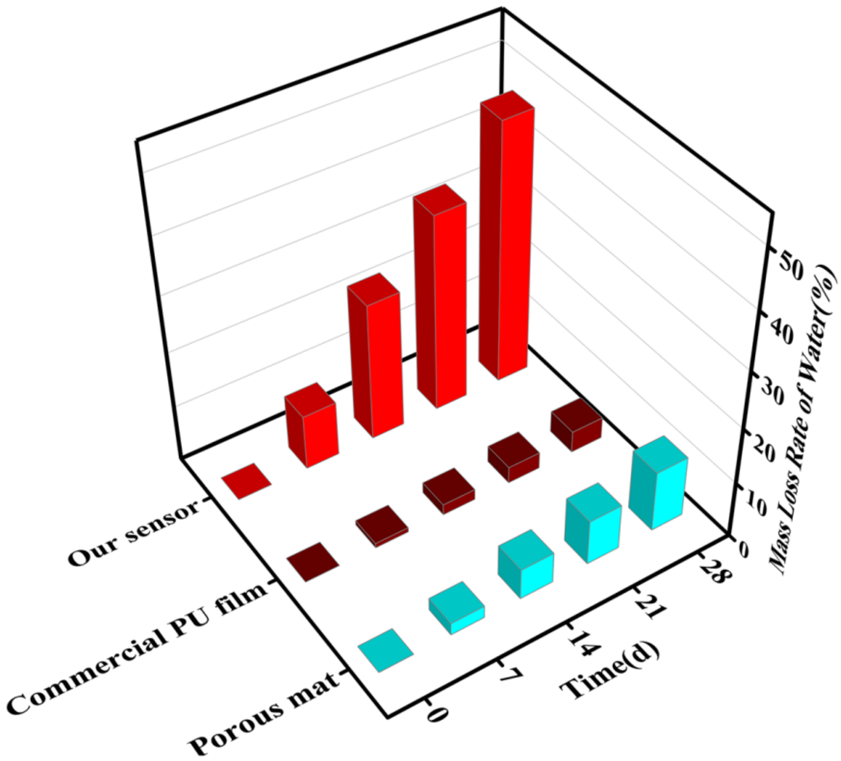


**Figure S16.** The permeability of our sensor, porous mat and commercial PU film.

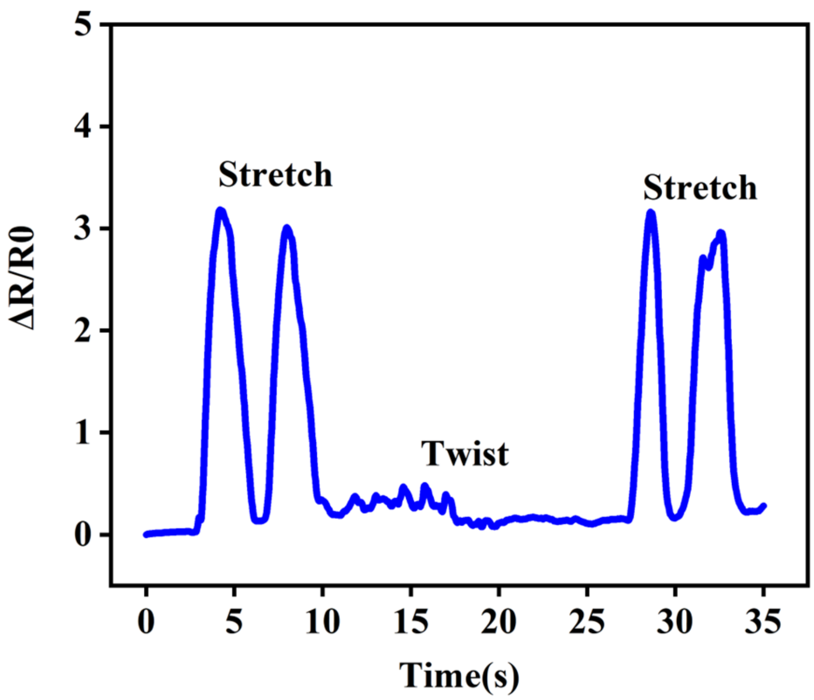


**Figure S17.** Strain response of the anti-interference test caused by off-axial twisting.

**Table S2.** Summary of recent wearable temperature sensors based on ionic gel

| Material | Sensitivity | Detection | Sensing | Reference |
|---|---|---|---|---|

| | | range | linearity | s |
|---|---|---|---|---|
| TPU/ILs | 2.73%·℃$^{-1}$ | 20-40 ℃ | - | [1] |
| TPU/ILs parallel fiber | 2.17%·℃$^{-1}$ | 30-100 ℃ | 0.998(30-40℃) | [2] |
| TPU/ILs | 2.10%·℃$^{-}$ | 30-50℃ | - | [9] |
| Silicone/ILs | 0.92%·℃$^{-1}$ | 25-100℃ | - | [10] |
| TPU/ILs | 1.20%·℃$^{-1}$ | -40-100℃ | 0.998(40-100℃) | [11] |
| TPU/ILs | 0.94%·℃$^{-1}$ | 30-80℃ | 0.998 | [12] |
| TPU/ILs | 1.55%·℃$^{-1}$ | 30-100℃ | 0.994 | This work |

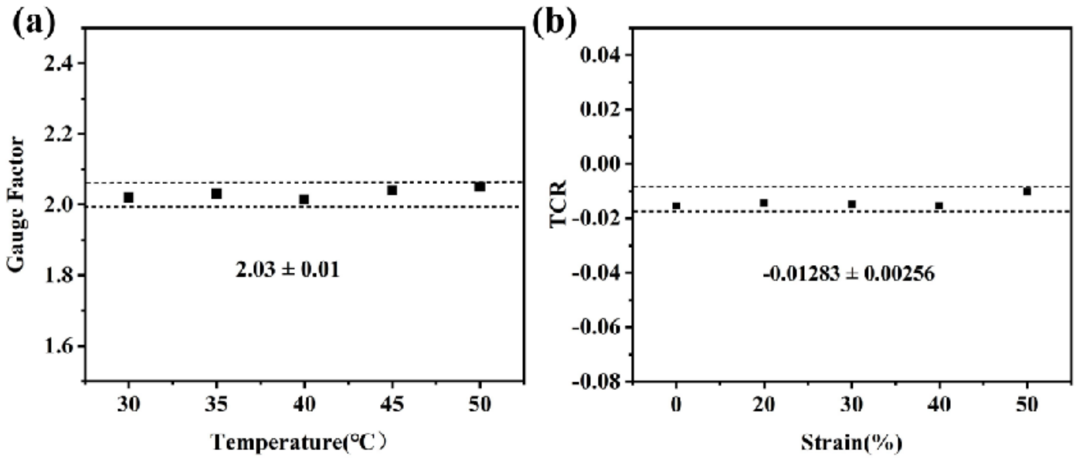


**Figure S18.** (a) GF changes with temperature, (b) TCR changes with strain.

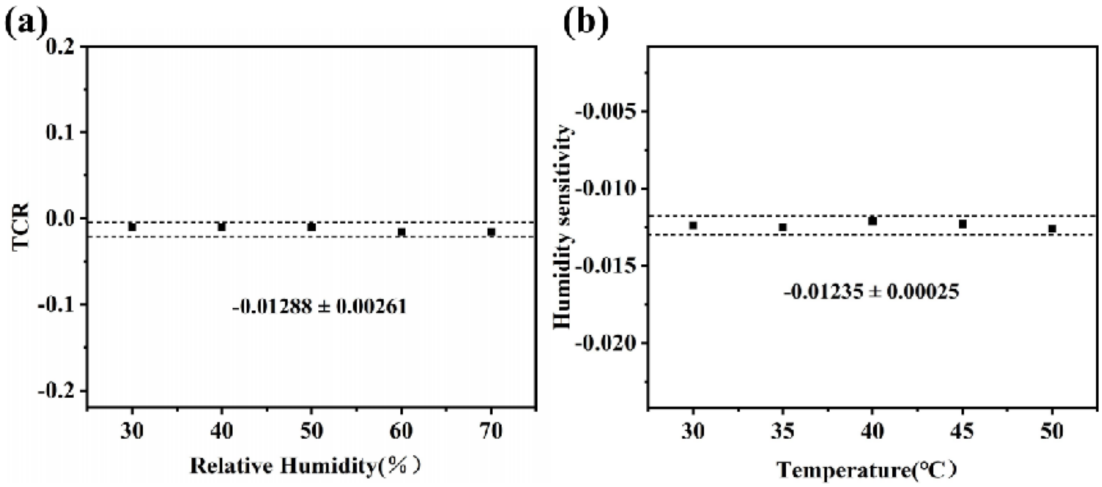


**Figure S19.** (a) TCR changes with humidity ,(b) Humidity sensitivity changes with temperature.

**Figure S20** shows schematic diagram of encoding the two-parameter signal such as strain and temperature. The components of strain and temperature signals with respect of time, is transformed into frequency signals. In this process, Fourier transform algorithm can be applied to encode the two-parameter signal based on the different response time of the device in temperature and strain sensing.

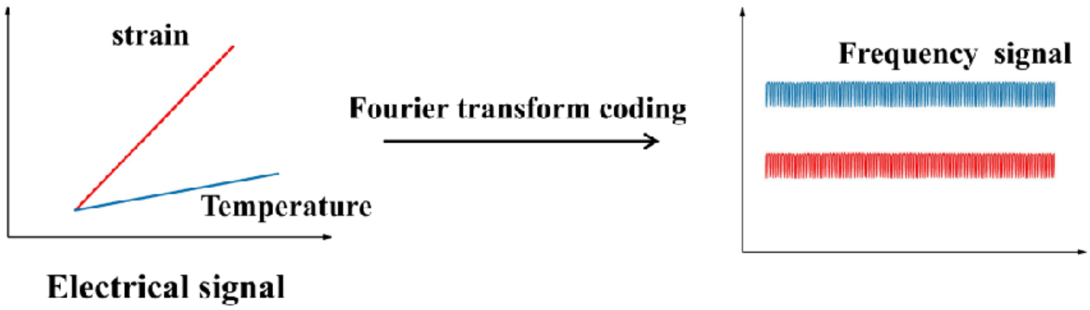


**Figure S20.** Schematic diagram of encoding the two-parameter signal such as strain and temperature

## References

[1] F. Li, H. Xue, X. Lin, C. Zhao, J. Li, H. Zhao, T. Zhang, *Advanced Materials Technologies* **2023**, 2300297.

[2] J. Chen, F. Wang, G. Zhu, C. Wang, X. Cui, M. Xi, X. Chang, Y. Zhu, *ACS Applied Materials & Interfaces* **2021**, 13, 51567.

[3] W. Y. Choi, J. H. Kwon, Y. M. Kim, H. C. Moon, *Small* **2023**, 2301868.

[4] S. Yang, C. Li, N. Wen, S. Xu, H. Huang, T. Cong, Y. Zhao, Z. Fan, K. Liu, L. Pan, *Journal of Materials Chemistry C* **2021**, 9, 13789.

[5] L. Chen, X. Chang, H. Wang, J. Chen, Y. Zhu, *Nano Energy* **2022**, 96, 107077.

[6] A. Khan, R. R. Kisannagar, S. Mahmood, W.-T. Chuang, M. Katiyar, D. Gupta, H.-C. Lin, *ACS Applied Materials & Interfaces* **2023**, 15, 42954.

[7] S. Xiang, X. He, F. Zheng, Q. Lu, *Chemical Engineering Journal* **2022**, 439, 135644.

[8] Y. Zhou, L. Zhao, Q. Jia, T. Wang, P. Sun, F. Liu, X. Yan, C. Wang, Y. Sun, G. Lu, *ACS Applied Materials & Interfaces* **2022**, 14, 55109.

[9] Y. Xu, L. Chen, J. Chen, X. Chang and Y. Zhu, ACS Applied Materials & Interfaces, 2**021**, 14, 2122-2131.

[10] S. Chen, H. Liu, S. Liu, P. Wang, S. Zeng, L. Sun and L. Liu, *ACS applied materials & interfaces*, 2018, 10, 4305-4314.

[11] N. Jiang, X. Chang, D. Hu, L. Chen, Y. Wang, J. Chen and Y. Zhu, *Chemical Engineering Journal*, 2021, 424, 130418.

[12] N. Jiang, H. Li, D. Hu, Y. Xu, Y. Hu, Y. Zhu, X. Han, G. Zhao, J. Chen and X. Chang, *Composites Communications*, 2021, 27, 100845.